Cavity swelling of RAFM steel under 792 MeV Ar-ions irradiation at 773 K *

SHEN Tie-Long(申铁龙)[1,2] WANG Zhi-Guang(王志光)[1;1)] YAO Cun-Feng(姚存峰)[1]
SUN Jian-Rong(孙建荣)[1] WEI Kong-Fang(魏孔芳)[1] ZHU Ya-Bin(朱亚滨)[1] PANG Li-Long(庞立龙)[1]
CUI Ming-Huan(崔明焕)[1,2] LI Yuan-Fei(李远飞)[1,2] MA Yi-Zhun(马艺准)[1]
SHENG Yan-Bin(盛彦斌)[1] GOU Jie(缑洁)[1]

[1] Institute of Modern Physics, Chinese Academy of Sciences, Lanzhou 730000, China
[2] University of Chinese Academy of Sciences, Beijing 100049, China

Abstract: China reduced-activation ferritic/martensitic steel is irradiated at 773 K with 792 MeV Ar-ions to fluences of 2.3×10^{20} and 4.6×10^{20} ions/m^2, respectively. The variation of the microstructures of the Reduced-activation ferritic/martensitic (RAFM) steel samples with the Ar-ion penetration depth is investigated using a transmission electron microscope (TEM). From analyses of the microstructure changes along with the Ar-ions penetrating depth, it is found that high-density cavities form in the peak damage region. The average size and the number density of the cavities depend strongly on the damage level and Ar-atom concentration. Swelling due to the formation of cavities increases significantly with an increased damage level, and the existence of deposited Ar-atoms also enhances the growth of the average size of the cavities. The effect of atom displacements and Ar-atoms on the swelling of the RAFM steel under high energy Ar-ion irradiation is discussed briefly.

Key words: RAFM steel, irradiation, TEM, cavity, swelling

PACS: 61.80.Jh, 68.37.Lp **DOI:** 10.1088/1674-1137/37/8/088201

1 Introduction

Radiation damage can influence the properties of materials such as the strength, ductility and dimensional stability. This can have a drastic impact on the safety and economic operation of fission and fusion reactors. It is well known that the radiation damage effect in nuclear reactors is a consequence of two basic types of damage, which include lattice atom displacement caused by irradiation and the foreign gas elements which are produced by (n, a) reaction. The inert gas helium has a vanishingly low solubility in metal and consequently is separated out to form small gas bubbles; moreover, helium also plays an important part in the initial nucleation of voids which subsequently grow by accumulation of vacancies [1]. On the other hand, it has been found that the helium atom plays an important role in stabilizing the 3D geometry for a small vacancy cluster than the 2D platelet geometry [2, 3]. It is therefore essential to acquire a comprehensive understanding of the effect of radiation damage and to use the information for the development of radiation-resistant alloys [4–6].

Reduced-activation ferritic/martensitic (RAFM) steel is considered to be a candidate structural material for advanced nuclear reactors because of its low activation, excellent mechanical property, good microstructure stability, and maturity as an industrial material [7–10]. During the last decade, a series of RAFM steels such as JLF, F82H, EUROFER97, and CLAM steels have been developed and investigated extensively [11–14]. The swelling behaviors of 3-18Cr ferritic steels under neutron irradiation were partly investigated in EBR-Ⅱ and FFTF [15, 16], respectively, for the absence of the corresponding fusion neutron source. So far, it is widely accepted that the lattice atom displacement and helium similar to that created in the structural materials of reactors can be reproduced separately or simultaneously by energetic ion beam bombardment [12]. Consequently, the synergistic effect of displacement damage and helium in swelling behaviors of the complex steels has been studied in triple/dual ions irradiation experiments [8, 17, 18]. However, with regard to the small penetration depths of ions in these experiments, the close proximity of the free surface as a defect sink makes it

Received 26 July 2012
∗ Supported by National Basic Research Program of China (973 Program, 2010CB832902) and National Natural Science Foundation of China (10835010, 91026002)
1) E-mail: zhgwang@impcas.ac.cn

almost impossible to quantitatively relate the damage retained within bulk material [12].

In the present study, microstructural changes of the China RAFM steel irradiated with 792 MeV Ar- ions at 773 K was investigated. On one hand, the penetration depth of high energy Ar-ions in steel was up to 130 μm and the influence of the free surface could generally be neglected. On the other hand, it was expected that argon could act as an analogue for helium. If a vacancy is present, both of the two inert gases will be strongly bound to the vacancy (with energy of a few eV), thus forming stable gas atom-vacancy cluster in the matrix [16]. Furthermore, energetic Ar- ions can produce displacement damage at a higher rate, namely a higher displacement damage level in a shorter time than He- ions. The objective of this study is first to investigate the dose dependence on the cavity swelling of the China RAFM steel at high temperature and second to study the synergistic effect of displacement damage and Ar concentration on cavity swelling.

2 The experiment

The sample used in this work is a China RAFM steel (CLAM steel, obtained from the Institute of Metal Research, CAS) with a size of 10 mm×15 mm×1 mm. The composition of the steel is given in Table 1. The samples were irradiated with 792 MeV Ar-ions at 773 K at the high temperature and stress materials research terminal of the Heavy Ion Research Facility of Lanzhou (HIRFL, China). The Ar-ion beam was scanned using two X-Y sets of magnets to a size of 15 mm×15 mm with homogeneity better than 95%. The irradiation was performed to two increasing fluences of 2.3×10^{20} and 4.6×10^{20} Ar-ions/m^2, respectively. During the irradiation, the average beam flux was about 6.4×10^{14} Ar-ions/m^2/s with a fluctuation within ±10%. The sample temperature was kept at 773 K with a fluctuations of 6 K in the conditions of the Ar-ion beam being turned on and turned off suddenly. Based on the calculation according to the SRIM2008 [19] (Fig. 1), the irradiation damage rate and the ratio of Ar-atom concentration to displacement per atom (dpa) at the peak damage region were approximately 2.5×10^{-5} dpa/s and 115 appm (10^{-6}) Ar/dpa, respectively. The peak damage level and Ar-atom concentration can reach up to about 9 dpa, 1035 appm Ar and about 18 dpa, 2070 appm Ar, corresponding to the fluences of 2.3×10^{20} and 4.6×10^{20} Ar-ions/m^2, respectively.

Table 1. Chemical composition of the RAFM steel (wt%).

Fe	Cr	C	Mn	Ta	W	V	Si	O	P
Bal	8.93	0.13	0.45	0.15	1.44	0.20	0.08	<0.002	<0.002

After irradiation, transmission electron microscope (TEM) observation of the cross-sectional specimen was performed with an FEI TECNAI G^2 F30 TEM at Lanzhou University. According to the obtained micrographs, the total volume and number density of cavities formed at different depths along the ion-incident direction were determined using thickness data of the specimen obtained by the contamination-spot separation method, as described in detail in Ref. [20], and then the corresponding bulk cavity swelling was deduced. The cavity swelling is often defined as:

$$S=V_c/(V-V_c), \quad (1)$$

where V_c is the total volume of the cavities induced by irradiation and V is the bulk of the specimen in the cavity region.

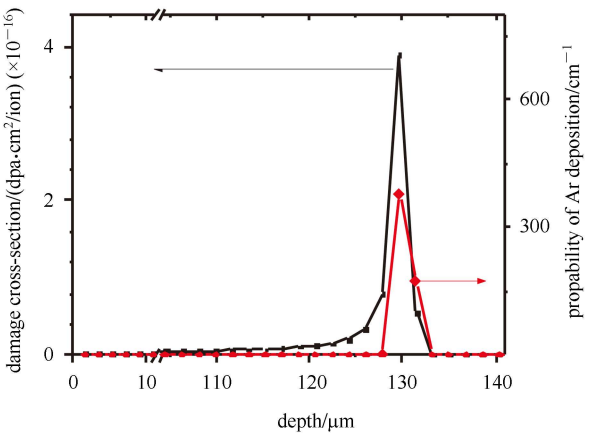

Fig. 1. Distributions of damage cross-section and Ar-atom deposition in RAFM steel evaluated by SRIM 2008.

3 Results and discussion

Figure 2(a) shows the microstructure of un-irradiated steel with a typical martensite lath structure containing martensite packets and lath boundaries formed during normalization. Moreover, the high-density precipitates, metal carbide (MC) and $M_{23}C_6$, formed during tempering were mostly located along the lath boundaries and inside the martensite lath. The number density of $M_{23}C_6$ and MC carbide particles were approximately 1.1×10^{19} m^{-3} and 1.19×10^{20} m^{-3}, respectively. The size of the $M_{23}C_6$ precipitates varied from 200 nm to 1500 nm, meanwhile, the size of the MC precipitates varied from 20 nm to 100 nm. The microstructures of the peak damage region in the samples irradiated to 2.3×10^{20} and 4.6×10^{20} Ar-ions/m^2 are shown in Figs. 2(b) and (c), respectively. Dense cavities formed in the peak damage regions of the irradiated samples are observed, as shown in Figs. 2(b) and (c). The average size of the cavities increases whereas the number of the cavities decreases slightly with increasing the irradiation fluence.

The maximum diameter (~130 nm) of cavities was found in the samples irradiated to 4.6×10^{20} Ar-ions/m^2 meanwhile the maximum cavity swelling (~4.29%) occurred.

In order to further understand the synergistic effect of the displacement damage and argon gas impurity on the cavity formation, the microstructures of the irradiated samples varying with the depths are discussed in detail. Fig. 3 shows TEM image of the depth distribution of the microstructures in the damage peak region of the sample irradiated to 2.3×10^{20} Ar-ions/m^2. The arrows show the incident direction of Ar-ions, and the parameters of the ion penetrating depth, the damage level and the deposited Ar concentration are also given in the figure. It can be seen that the size and the density of the formed cavities have a strong dependence on the damage level and the deposited Ar concentration, as shown in Figs. 3(a)–(f). The largest size cavities (up to 70 nm) produced by irradiation are observed at the depth of approximately 130 μm beneath the incident surface (Fig. 3(c)). The size distributions of the cavities at different depth with different damage levels and Ar concentrations are given in Fig. 4. A typical size distribution of the cavities near the peak damage region containing a high density of cavities at small sizes and another larger size ones with relatively few number is shown in Figs. 4(c) and 4(g). Such a size distribution provides evidence of a possible coarsening mechanism of the cavities via dislocation bias driven growth [21, 22].

Furthermore, the average size of the cavities, the cavity number density as well as the deduced cavity swelling varying with the Ar-ions penetrating depth are demonstrated in Fig. 5. It is noticeable that, the average

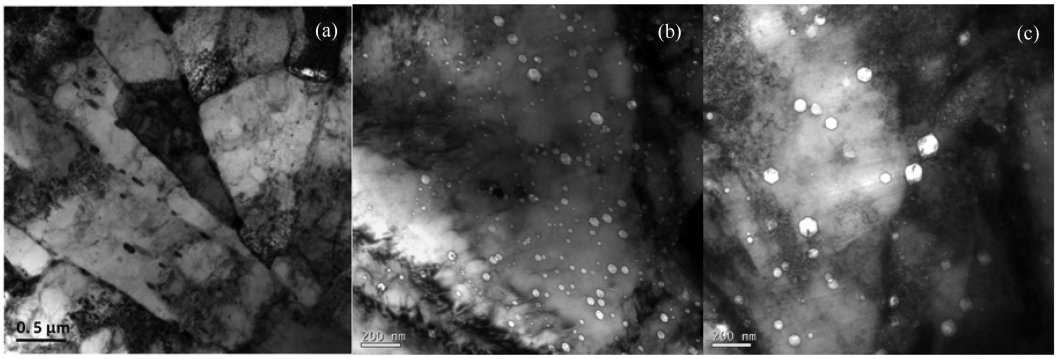

Fig. 2. Typical bright field images of RAFM steel at different conditions: (a) un-irradiated; (b) 2.3×10^{20} and (c) 4.6×10^{20} Ar-ions/m^2.

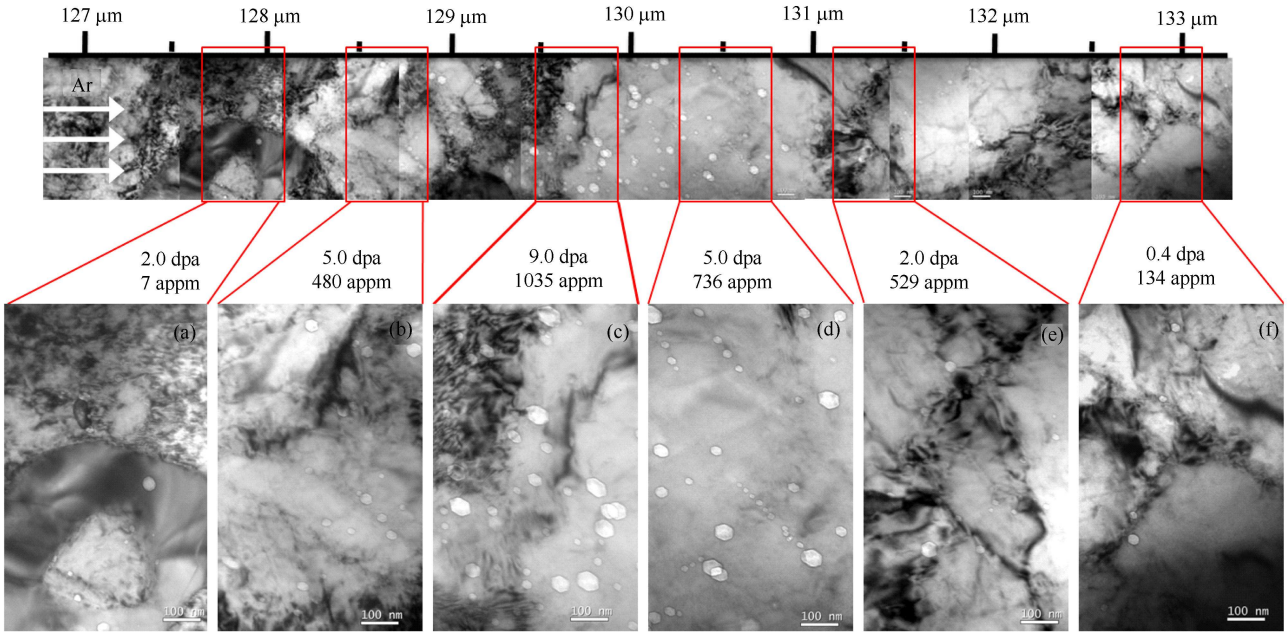

Fig. 3. Typical cross-sectional micrographs of the peak damage region in the RAFM steel irradiated to 2.3×10^{20} Ar-ions/m^2.

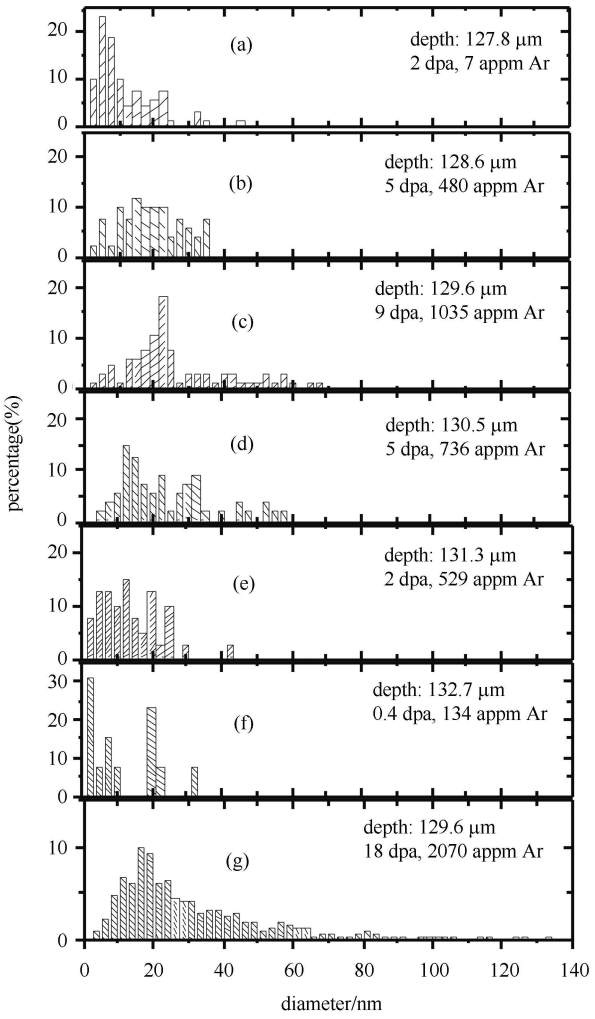

Fig. 4. Percentage of the cavity number versus the cavity size at different depths. The corresponding damage level and Ar-atom concentration are given in the figure.

diameter and number density of the cavities as well as the deduced cavity swelling value all peak at a depth of around 130 μm. The maximum swelling value is about 2.7% near the peak damage region with the damage level and Ar-atom concentration of 9 dpa and 1035 appm, respectively. Since the highest displacement damage rate occurs in the peak damage region for single ion irradiation, a high density of dislocations is observed at the depth of 129.4 μm, as shown in Fig. 3. According to the theoretical model of Stoller and Odette [23], a higher total dislocation density in the peak damage region could reduce the vacancy supersaturation and consequently result in lower void nucleation rate. Therefore, the maximum swelling does not occur in the peak displacement damage region but in the peak Ar-atom concentration region.

Figure 6 shows a summary of the cavity swelling values varying with the damage level and the corresponding Ar-atom concentration values are also labeled. The cavity swelling value increases from ∼0.06% to a maximum of ∼4.29% when the damage level increases from 0.36 to 18 dpa. The dose dependence of the swelling (the curved line) is consistent with the theoretical prediction by Mansur [24]. As can be seen, there are three regions of dose dependence according to Q, which is the ratio of the dislocation sink strength to cavity sink strength. At low doses ($Q \gg 1$), the dislocations are the dominant sink and result in lower swelling rate. At high doses ($Q \ll 1$), the cavities typically become the dominant sinks when the dislocation density is maintained constant and this case indicates the situation where most point defects of either type are absorbed by cavities, essentially resulting in efficient annihilation of interstitials and vacancies with little net absorption. Therefore, the swelling rate cannot increase rapidly under the conditions of $Q \gg 1$ and $Q \ll 1$ [22].

In addition, taking into account the comparison among the following points (2 dpa, 7 appm Ar), (2 dpa, 529 appm Ar), (5 dpa, 480 appm Ar) and (5 dpa, 736 appm Ar), it is found that, for the same damage level, the cavity swelling increases with increasing the deposited Ar concentration. The comparison between the points (2 dpa, 529 appm Ar) and (5 dpa, 480 appm Ar) indicates

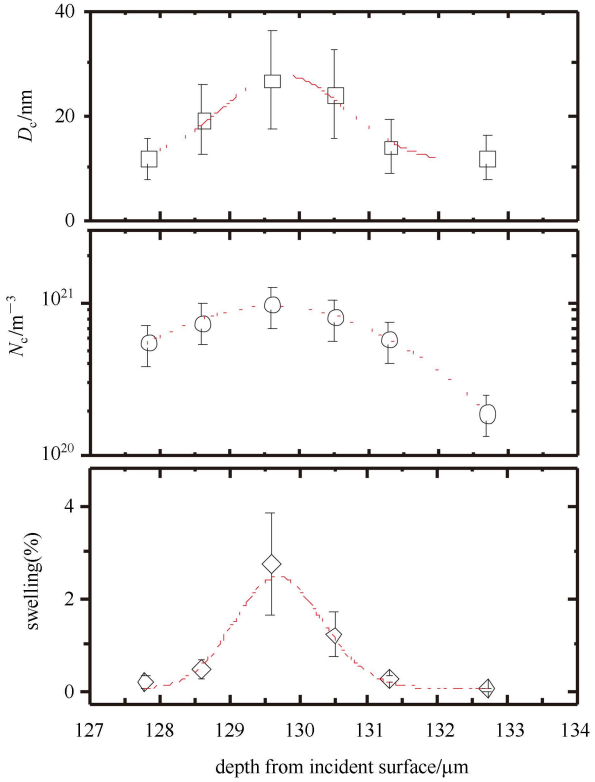

Fig. 5. (color noline) The depth distributions of average diameter and number density of cavities as well as the deduced cavity swelling of RAFM steel irradiated to 2.3×10^{20} Ar-ions/m^2.

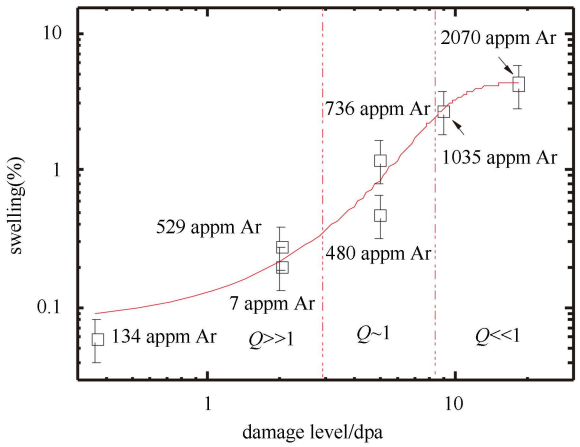

Fig. 6. (color online) The cavity swelling varying with the damage level. The corresponding Ar-atom concentration values are given in the figure.

that the cavity swelling for a given deposited Ar concentration increases with increasing the damage level. It should be noted that the immobile inert gas atoms may act to enhance the cavities nucleation and stabilize a cavity embryo by the gas pressure [12, 13, 25, 26]. For a lower dpa value and lower Ar-atom concentration, the cavity nucleates via the multi-atomic nucleation model, and then grows due to the internal argon gas pressure. Thus, this condition results in the weak swelling by lacking excess vacancies. With increasing the dpa value, the cavity embryos can absorb a sufficient number of Ar atoms or vacancies introduced by the irradiation via a vacancy mechanism at high temperature and grow to larger ones that lead to a larger swelling. However, for high dpa level and large Ar-atom concentration, the coexistence of the gas-driven and the vacancy supersaturation- driven stages lead to the appearance of larger voids (∼130 nm in diameter) via dislocations bias driven growth. Similar cavity size distributions were reported in the study of T92 and JLF-1steels with Ne-ion and Fe plus He-ions dual-beam irradiations [17, 18, 21].

4 Summary

The home-made RAFM steel irradiated with 792 Ar-ions at 773 K to 2.3×10^{20} and 4.6×10^{20} ions/m^2 was investigated by using TEM measurement. From the analyses of microstructure change along with the depth beneath the ion incident surface, we found high-density cavities with a size distribution via dislocations bias driven growth in the Ar-ion irradiated samples. The dose dependence on cavity swelling of the China RAFM steel at high temperature was discussed and there was a synergistic effect in the cavity formation during the Ar-ion irradiation. The average size and the number density of the cavities depend strongly on the damage levels and Ar-atoms concentrations. The cavity swelling value increased from ∼0.06% to a maximum of ∼4.29% with the damage level increased from 0.36 to 18 dpa. For the same damage level, the higher the Ar-atom concentration, the larger the cavity swelling produced in the sample.

The authors would like to thank the staff of HIRFL-SSC in IMP for their collaboration during the Ar-ion irradiation experiment.

References

1 Nelson R S, Mazey D J, Hudson J A. J. Nucl. Mater., 1970, **37**: 1
2 Zinkle S J, Lee E H. Metallurgical Transactions A, 1990, **21**: 1037
3 Zinkle S J, Seitzman L E, Wolfer W G. Philos. Mag. A, 1987, **55**: 111; Zinkle S J, Wolfer W G, Kulcinski G L et al. Philos. Mag. A, 1987, **55**: 127
4 Ullmaier H, Schilling W. Radiation Damage in Metallic Reactor Materials, Physics of Modern Materials, 1980, 1
5 Schilling W, Ullmaier H. Physics of Radiation Damage in Metals. In: Nuclear Materials, Materials Science and Technology, 1993, **10**: Weinheim and New York: VCH Verlag.
6 Zinkle S J, Busby J T. Mater. Today, 2009, **12**: 12
7 Johnston W G, Rosolowski J H, Turkalo A M et al. J. Nucl. Mater., 1974, **54**: 24
8 van der Schaaf B, Gelles D S, Jitsukawa S et al. J. Nucl. Mater., 2000, **283–287**: 52
9 Klueh R L, Gelles D S, Jitsukawa S et al. J. Nucl. Mater., 2002, **307–311**: 455
10 Zinkle S J, Victoria M, Abe K. J. Nucl. Mater., 2002, **307–311**: 31
11 Wakai E, Kikuchi K, Yamamoto S et al. J. Nucl. Mater., 2003, **318**: 267
12 Tanigawa H, Ando M, Katoh Y et al. J. Nucl. Mater., 2001, **297**: 279
13 TONG Z, DAI Y. J. Nucl. Mater., 2010, **398**: 43
14 HUANG Q, LI J, CHEN Y et al. J. Nucl. Mater., 2004, **329–333**: 268
15 Toloczko M B, Garner F A, Eiholzer C R. J. Nucl. Mater., 1994, **212–215**: 604
16 Sencer B H, Garner F A. J. Nucl. Mater., 2000, **283–287**: 164
17 Ogiwara H, Sakasegawa H, Tanigawa H et al. J. Nucl. Mater., 2002, **307–311**: 299
18 Yutani K, Kishimoto H, Kasada R et al. J. Nucl. Mater., 2007, **367–370**: 423
19 Ziegler J F, Biersack J P, Littmark U. The Stopping and Range of Ions in Solids. Pergamon, New York: 1985, http://www.srim.org
20 Williams D B, Carter C B. Transmission Electron Microscopy, Springer Science+ Business Media, LLC. New York: 2009, 670
21 ZHANG C H, JANG J, Kim M C et al. J. Nucl. Mater., 2008, **375**: 185
22 Mansur L K. J. Nucl. Mater., 1994, **216**: 97
23 Stoller R E, Odette G R. Radiation Induced Changes in Microstructure. Thirteenth Conf., ASTM STP 955, Eds. Garner F A, Packan N H, Kumar A S. ASTM, Philadelphia, 1987. 371–392
24 Mansur L K. J. Nucl. Mater., 1993, **206**: 306
25 Trinkaus H. Radiat. Eff., 1983, **78**: 189
26 Mansur L K, Coghlan W A. J. Nucl. Mater., 1983, **119**: 1